Nonlinear Dispersive Modeling of Electron Devices Oriented to GaN Power Amplifier Design

Antonio Raffo, *Member, IEEE*, Valeria Vadalà, *Student Member, IEEE*, Dominique M. M.-P. Schreurs, *Senior Member, IEEE*, Giovanni Crupi, Gustavo Avolio, Alina Caddemi, and Giorgio Vannini, *Member, IEEE*

***Abstract*—This paper presents a new modeling approach accounting for the nonlinear description of low-frequency dispersive effects (due to thermal phenomena and traps) affecting electron devices. The theoretical formulation is quite general and includes as particular cases different models proposed in the literature. A large set of experimental results, oriented to microwave GaN power amplifier design, is provided to give an exhaustive validation under realistic device operation.**

***Index Terms*—Field-effect transistors (FETs), microwave amplifiers, nonlinear distortion, nonlinear circuits, semiconductor device modeling.**

I. Introduction

THE DESIGN of power amplifiers represents a fundamental topic for the microwave community, as clearly demonstrated by the increasing number of books [1]–[5] dedicated to this issue published in recent years. This is justified by the important role that power amplifiers play in microwave systems (e.g., satellite front-ends, base stations, mobile phones). The advent of GaN technology [6]–[8] has provided new stimuli in this design field foreseeing unbelievable performance in terms of power density, available power, drain efficiency, high-voltage, and high-temperature operation.

A widely adopted tool for power amplifier design is represented by load–pull measurements [9]–[14], based on both passive or active load synthesis. Such a type of measurement system, being able to synthesize the optimum load and source conditions at the design frequency, supplies the designer with very useful information. Nevertheless, a model is needed for different reasons: simulating the device behavior at the intrinsic device ports to assess the actual load-line at the device resistive core (this is a fundamental issue, especially for high-efficiency amplifier classes), verifying process dispersion influence on device performance, investigating device stability, and wideband behavior, and so on.

The identification of an electron device model, which aims to be a powerful design tool under different classes of amplifier operation, cannot neglect the dispersion presented by the electron device current/voltage characteristics related to traps and thermal effects [15]–[19]. These effects have to be accurately characterized, especially when new, and as consequence, immature technologies are considered (e.g., GaN and InP) since low-frequency (LF) dispersion unquestionably represents a bottleneck in device performance.

Different models have been proposed by the microwave community in the last 20 years to correctly account for LF dispersion: from the simplest, and probably the first one, [20] proposed by Camacho-Penalosa (which adopts an *RC* network) to more complex models based on lookup-table approaches (e.g., [21] and [22]). The major problem related to the last mentioned approaches is that, despite the great level of accuracy obtainable, they are rarely used by designers due to the considerable simulation time required and convergence problems.

As a matter of fact, models that are based on bias-independent parameters [23]–[29] represent the optimum compromise between accuracy and simulation time. Such a kind of description is typically based on simplifying approximations of the complex phenomena related to LF dispersion, as a consequence, it can be inadequate when new technologies (where dispersive effects play a major role) have to be investigated. In this paper, a very general analytical formulation will be introduced for the description of LF dispersion affecting microwave devices, which clearly demonstrates as different approaches [24]–[27] published in recent years, can be enhanced in order to obtain acceptable prediction capability also in the presence of strong dispersion. In particular, the proposed formulation, which is justified both by theoretical and empirical considerations, allows to identify a limited set of bias-independent parameters, which guarantees an excellent compromise between accuracy and simulation time. As a consequence, this modeling approach is particularly suitable for the design of power amplifiers based on the latest device technologies (e.g., GaN).

This paper is organized as follows. Section II describes the theoretical model formulation and discusses the effects of the correction terms introduced. In Section III, a large variety of experimental results is provided to definitely validate the proposed approach. Finally, conclusions are drawn in Section IV.

Manuscript received July 16, 2009; revised December 11, 2009. First published March 08, 2010; current version published April 14, 2010. This work was supported in part by the Italian Ministry of Instruction, University and Research (MIUR), the Research Foundation Flanders (FWO–Vlaanderen), IMT-ARSEL Project prot. RBIP06R9X5, and the CMOGAN Project through the contribution of the Italian Ministero degli Affari Esteri, Direzione Generale per la Promozione e la Cooperazione Culturale.

A. Raffo, V. Vadalà, and G. Vannini are with the Department of Engineering, University of Ferrara, 44100 Ferrara, Italy (e-mail: antonio.raffo@unife.it; valeria.vadala@unife.it; Giorgio.Vannini@unife.it).

D. M. M.-P. Schreurs and G. Avolio are with the Electronic Engineering Department, Katholieke Universiteit Leuven, B-3001 Leuven, Belgium (e-mail: dominique.schreurs@esat.kuleuven.be; gustavo.avolio@esat.kuleuven.be).

G. Crupi and A. Caddemi are with the Dipartimento di Fisica della Materia e Ingegneria Elettronica, University of Messina, 98166 Messina, Italy (e-mail: giocrupi@ingegneria.unime.it; caddemi@ingegneria.unime.it).

Color versions of one or more of the figures in this paper are available online at http://ieeexplore.ieee.org.

Digital Object Identifier 10.1109/TMTT.2010.2041572

II. Nonlinear Modeling of LF Dispersion

A. Model Formulation

When dealing with operating frequencies where the dynamic effects associated to charge storage variations and/or finite transit times can be neglected (i.e., LF dynamic regime), the vector $\underline{i}$ of the instantaneous currents of a microwave field-effect transistor (FET) device (i.e., MESFET or HEMT) can be formulated as

$$\underline{i} = \begin{bmatrix} i_g(t) \\ i_d(t) \end{bmatrix} = \begin{bmatrix} f_g(\underline{v}, X_\vartheta) \\ f_d(\underline{v}, X_T, X_\vartheta) \end{bmatrix} \tag{1}$$

where $\underline{v}$ is the vector of the instantaneous voltages at the device ports, while X_ϑ and X_T are state variables describing the device thermal and trap state, respectively. The thermal state influences the gate current as demonstrated by different papers devoted to the thermal resistance characterization (e.g., [30]), which exploit the gate *I/V* characteristic as a thermal sensor. On the other hand, the major influence of the trap and thermal states on the drain current has been widely discussed and demonstrated in the literature [15]–[29].

By considering microwave single- or two-tone[1] device operation with frequency components lying above[2] the cutoff frequencies of the LF dispersive effects, the device thermal and trap states can be considered as frozen to their average values since they cannot change according to instantaneous signal variations. In this operating regime, (1) can be rewritten as

$$\underline{i} = \begin{bmatrix} i_g(t) \\ i_d(t) \end{bmatrix} = \begin{bmatrix} f_g\left(\underline{v}, X_\vartheta^0\right) \\ f_d\left(\underline{v}, X_T^0, X_\vartheta^0\right) \end{bmatrix} \tag{2}$$

where X_ϑ^0 and X_T^0 represent average values. It has been widely demonstrated, both by theoretical considerations [21]–[28] and experimental results [15], [16], that these two state variables, in the particular operation considered, can be assumed dependent only on the vector $\underline{V}^0$ of the average values of the voltages applied at the device ports and on the average value of the channel temperature ϑ_j^0

$$\begin{aligned} \vartheta_j^0 &= \vartheta_c + R_\vartheta P^0 \\ P^0 &= \frac{1}{T}\int_0^T p(t)dt \end{aligned} \tag{3}$$

where ϑ_c is the case temperature, R_ϑ is the thermal resistance, P^0 is the average power dissipated, and $p(t)$ is the instantaneous power. From the previous considerations, and considering (3), it follows that the trap and thermal state variables can be expressed as

$$\begin{bmatrix} X_T^0 \\ X_\vartheta^0 \end{bmatrix} = \begin{bmatrix} f_T\left(\underline{V}^0, \vartheta_j^0\right) \\ f_\vartheta\left(\vartheta_j^0\right) \end{bmatrix} = \begin{bmatrix} f_T(\underline{V}^0, P^0, \vartheta_c) \\ f_\vartheta(P^0, \vartheta_c) \end{bmatrix} \tag{4}$$

where the dependence of the trap state on the thermal state has also been accounted for [18], [23].

[1]In the case of two-tone excitation, the tone spacing has to be greater than the highest cutoff frequency associated to LF dispersive effects.

[2]Practically all of the models available in the literature do not deal with the problem of accurate modeling of the dynamic device response within the "trap bandwidth" and usually account for the transition between dc and LF operation above trap cutoff through a single time-constant *RC* network.

This paper is focused on the description of the device drain current, whereas the gate current dispersion will be neglected. Such an approximation is justified since the gate current thermal dependence does not greatly affect model prediction capability under typical power amplifier operation. As a matter of fact, to put in evidence such a dispersion, important variations of the case temperature (i.e., 40 °C–50 °C) and/or high dissipation bias conditions (e.g., setting the gate bias voltage V_g^0 at the forward conduction threshold of the gate/source diode and the drain bias voltage V_d^0 in the saturation region) are needed: such operating regimes are clearly not particularly interesting in power amplifier design.

By considering (4), the drain current equation in (2) can be expressed as

$$i_d(t) = f_d\left(\underline{v}, X_T^0, X_\vartheta^0\right) = F(\underline{v}, \underline{V}^0, P^0, \vartheta_c). \tag{5}$$

The algebraic function F can be defined in different ways, nevertheless, it has to satisfy some physical requirements. A most important one being that, under dc operation, it has to coincide with the device static characteristics $F(\underline{v}, \underline{V}^0, P^0, \vartheta_c)|_{\rm dc} = F_{\rm dc}(\underline{v}, \vartheta_c)$. For such a reason, it is quite intuitive to adopt a formulation that describes the dynamic current deviations with respect to dc by modifying the device dc characteristic

$$\begin{aligned} i_d(t) &= F(\underline{v}, \underline{V}^0, P^0, \vartheta_c) \\ &= \left[1 + \Delta_m(\underline{v}, \underline{V}^0, P^0)\right] \cdot F_{\rm dc}(\underline{v_x}, \vartheta_c) \\ \underline{v_x} &= \begin{bmatrix} v_{gx}(t) \\ v_{dx}(t) \end{bmatrix} \\ &= \begin{bmatrix} v_g(t) + \Delta_g(\underline{v}, \underline{V}^0, P^0) \\ v_d(t) \cdot \left(1 + \Delta_d(\underline{v}, \underline{V}^0, P^0)\right) \end{bmatrix} \end{aligned} \tag{6}$$

where $\underline{v_x}$ is the vector of the modified voltages, whereas the correction terms Δ_m, Δ_g, and Δ_d, account for the drain current deviations related to LF dispersion.

The particular expressions adopted to "modify" the dc characteristic are justified both by considering previous approaches [23]–[27] and by empirical observations; moreover, their validity is confirmed by the experimental results provided in the following. In particular, the formulation adopted for the modified drain voltage v_{dx} allows to satisfy the physical constraint that, under LF operation, the drain current has to be null when the instantaneous drain voltage is null. Moreover, the dependence on the case temperature (which is considered constant under device operation) has been included only in the dc characteristic $F_{\rm dc}$.

The correction terms Δ can be conveniently expressed as a function of purely dynamic terms defined as the difference between the instantaneous values of the controlling electrical quantities and the corresponding average values

$$\begin{aligned} \Delta_m(t) &= f_{\Delta m}(\delta_{vg}, \delta_{vd}, \delta_p) \\ \Delta_g(t) &= f_{\Delta g}(\delta_{vg}, \delta_{vd}, \delta_p) \\ \Delta_d(t) &= f_{\Delta d}(\delta_{vg}, \delta_{vd}, \delta_p). \end{aligned} \tag{7}$$

with

$$\begin{aligned} \delta_{vg} &= v_g(t) - V_g^0 \\ \delta_{vd} &= v_d(t) - V_d^0 \\ \delta_p &= p(t) - P^0. \end{aligned} \tag{8}$$

An analytical formulation of the functions f_Δ can be obtained by adopting a Taylor expansion. By focusing on the 1-D case for the sake of simplicity, we can write for any of the f_Δ functions

$$f_\Delta(\delta_i) = \sum_{k=0}^{\infty} \left[\left. \frac{\partial f^k}{\partial \delta_i} \right|_{\delta_i=\delta_{i0}} \cdot \frac{(\delta_i - \delta_{i0})^k}{k!} \right] = \sum_{r=0}^{\infty} \alpha_r \delta_{io}^r + \sum_{p=1}^{\infty}\sum_{q=1}^{\infty} \alpha_{pq} \delta_i^p \delta_{i0}^q + \sum_{n=1}^{\infty} \alpha_n \delta_i^n. \quad (9)$$

As previously observed, under dc operation, the function F has to coincide with the dc one in (6); this implies that, under dc operation, the correction terms $\Delta = f_\Delta(\delta_i)$ have to be null. Such a condition can be easily imposed, without introducing any approximation, by setting δ_{i0} equal to 0 in (9); thus, for the multidimensional case, the generic f_Δ function reduces to

$$f_\Delta(\delta_1, \delta_2, \ldots, \delta_n) = \sum_{\substack{n1=0 \\ (n1+\ldots+nn\neq 0)}}^{\infty} \cdots \sum_{nn=0}^{\infty} \alpha_{n1,\ldots,nn} \delta_1^{n1} \cdot \ldots \cdot \delta_n^{nn} \quad (10)$$

and, finally, the correction terms become

$$\begin{aligned} \Delta_m(t) &= \sum_{\substack{gm=0 \\ (gm+dm+pm\neq 0)}}^{n1} \sum_{dm=0}^{n2} \sum_{pm=0}^{n3} \alpha^m_{gm,dm,pm} \delta_{vg}^{gm} \delta_{vd}^{dm} \delta_p^{pm} \\ \Delta_g(t) &= \sum_{\substack{gg=0 \\ (gg+dg+pg\neq 0)}}^{n4} \sum_{dg=0}^{n5} \sum_{pg=0}^{n6} \alpha^g_{gg,dg,pg} \delta_{vg}^{gg} \delta_{vd}^{dg} \delta_p^{pg} \\ \Delta_d(t) &= \sum_{\substack{gd=0 \\ (gd+dd+pd\neq 0)}}^{n7} \sum_{dd=0}^{n8} \sum_{pd=0}^{n9} \alpha^d_{gd,dd,pd} \delta_{vg}^{gd} \delta_{vd}^{dd} \delta_p^{pd} \end{aligned} \quad (11)$$

where the $\alpha_{x,y,z}$ coefficients are the bias-independent model parameters to be identified.

Equation (6) and the correction terms (11) define a general-purpose nonlinear model for dispersive effects, which satisfies physical and experimental evidence. It can be applied starting from any possible description of an electron device dc characteristics (e.g., analytical, lookup-table based, etc.). Different model formulations reduce to (6) and (11) under simplifying assumptions [24]–[27].

In the next paragraph, the effects of the correction terms (11) are analyzed in order to derive guidelines for the optimal choice of the model parameters.

B. Correction Terms Effects

The deviations existing between static and dynamic device output characteristics, measured at operating frequencies where the nonlinear dynamic effects associated to charge storage variations can be totally neglected, are schematically shown in Fig. 1. In this figure, the knee walkout (KW) of the dynamic characteristics, the negative slope (NS) of the dc characteristic in the saturation region, and the saturation current collapse (CC)[3] are put in evidence. All these effects globally contribute to decrease device performance under dynamic operation, and as a consequence, have to be correctly accounted for.

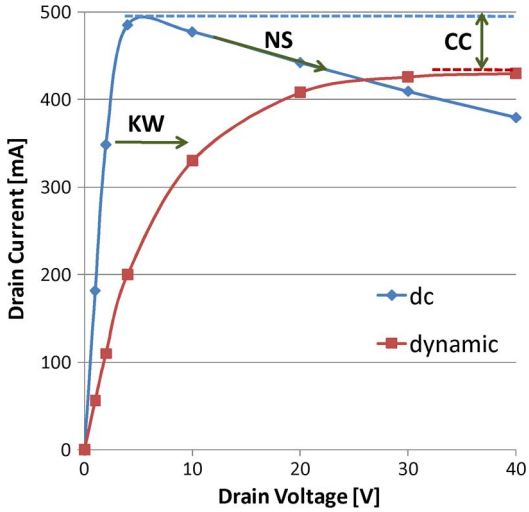

Fig. 1. Schematic representation of the differences existing between dc and dynamic device characteristics.

The KW can be accurately predicted by modeling the different slopes shown by the dynamic characteristics in the linear region. Such a kind of discrepancy can be simply accounted for by a correction in the drain voltage dependence of the static characteristic, i.e., by the correction term[4] Δ_d in (6). It has been largely demonstrated (e.g., [16]–[18]) that the KW monotonically increases by increasing the drain bias voltage V_d^0; as a consequence, the contribution δ_{vd} has to be necessarily considered. If a significant dependence on the gate bias voltage is present, the contribution δ_{vg} should also be included. Since the correction term Δ_d only accounts for small deviations of the characteristic slope in the linear region, it is meaningless to exceed in its polynomial degree: a first-order expansion is typically adequate.

When dynamic operation is considered, the device thermal state is defined by (3); thus, differently from the dc ones, the dynamic characteristics do not show any NS in the saturation region: this behavior can be accounted for through the multiplying correction term Δ_m. Since thermal effects are mainly responsible for such a deviation, the contribution δ_p has to be introduced. It can be observed that dynamic characteristics measured under the same thermal state (e.g., under no power dissipation), but starting from different bias conditions, can show different slopes in the saturation region [15]–[17]. In this respect, it is necessary to also introduce the contributions deriving from the deviations δ_{vg} and δ_{vd}. Since the correction term Δ_m has only to account for deviations related to the characteristic slope in the saturation region, also in this case, it is unfruitful to exceed in its

[3]The CC can be also defined with respect to a pulsed characteristic measured by exploiting a bias condition which guarantees both no power dissipation and channel formation (e.g., $V_g^0 = 0$ V and $V_d^0 = 0$ V), nevertheless the definition adopted here is more congruent with the model theoretical formulation.

[4]This term is conceptually similar to the effect of a parasitic drain resistance, which, causing a voltage drop, is able to modify the slope of the dc characteristics in the linear region.

polynomial degree, and a first-order expansion can be adopted. It should be noticed that in [24] and [27] the authors obtained very good prediction capability without adopting such a term. This is coherent with the low-power device considered there, as can be seen looking at the dc characteristics, which do not show any NS.

The CC essentially arises from the presence of surface trap states [16], [17] and is accounted for by the last correction term Δ_g. Such a phenomenon is strongly dependent on both the bias condition and the device thermal state so all the δ-deviations have to be exploited. Moreover, due to its very complex behavior, when new device technologies are investigated, a high-order polynomial degree may be required.

The theoretical formulation (6), (11) clearly shows that the *mixed correction terms*, arising from the mixed terms in the Taylor expansion, have to be accounted for too. These terms were completely and arbitrarily neglected in [26] and [27] and this is probably the reason why a high-order polynomial was necessary, in those particular cases, for the correction term Δ_d. Nevertheless, careful considerations are needed before increasing the order of such a correction term since, beside the motivations previously discussed, if Δ_d becomes smaller than -1, the drain current goes negative in correspondence of positive drain voltage values. Obviously such a behavior is completely unphysical under LF operation. As a matter of fact, it is strongly suggested to maintain the polynomial order of the correction term Δ_d as low as possible.

Since the theoretical formulation proposed here is based on bias-independent parameters, it could be easily identified, through least square algorithms, by exploiting LF small-signal measurements carried out under different bias conditions at a single frequency (e.g., 40 MHz) above the cutoff of LF dispersive effects (the measurement number depending on the number of parameters exploited). As a matter of fact, since the proposed approach is oriented to nonlinear amplifier design, it is preferable to base the identification procedure on large-signal measurements carried out under pulsed [15] and\or sinusoidal [31] excitations.

III. Experimental Results

The presented model formulation was exploited to characterize the nonlinear dynamic behavior of a 0.7×800 μm^2 GaN HEMT device. As a first step, a suitable parasitic network was extracted by adopting a conventional technique based on "cold" scattering parameter measurements ($V_d^0 = 0$ V).

In the characterization phase, an LF time-domain load–pull measurement system based on sinusoidal excitations at 2 MHz [31] was adopted. Two 50-Ω signal sources allow to impose the amplitudes of the incident-waves applied at the gate and drain ports and their relative phase. As previously said, the operating frequency has been chosen above the cutoff of LF dispersive effects, but low enough to neglect dynamic effects related to the device reactive parasitic elements and the high-frequency capacitive effects. Different papers (e.g., [14]) document the influence of dispersive phenomena (essentially related to thermal effects) at frequencies above the frequency exploited in this paper. Nevertheless, Fig. 2 reports measurements carried out

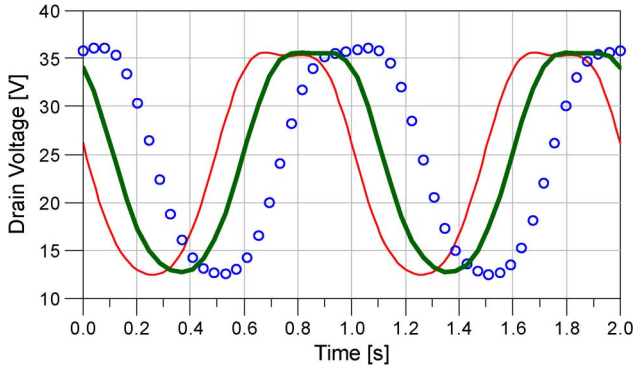

Fig. 2. Measurements carried out at different frequencies to assess the correctness of the chosen characterization frequency (thin line: 2 MHz, thick line: 10 MHz, circles: 20 MHz). The waveform time scale has been properly normalized to fit two periods; moreover, a time shift has been introduced between waveforms to make the differences appreciable.

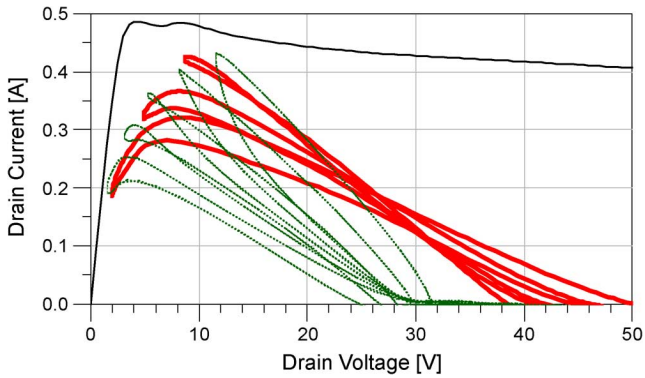

Fig. 3. Measurements performed on the GaN device-under-test (DUT) at 2 MHz, the two sets have the same drain bias condition ($V_d^0 = 25$ V) and different gate bias values $V_g^0 = -2$ V (continuous line) and $V_g^0 = -4$ V (dotted line). Class-A operation: amplitude of the input incident signal $A_g = 1$ V, amplitude of the output incident signal $3.1\ \text{V} \leq A_d \leq 11$ V, relative phase $\Delta\phi = 180°$. Class-B operation: $A_g = 2$ V, $1.4\ \text{V} \leq A_d \leq 9.8$ V, $\Delta\phi = 180°$. The dc characteristic for $v_g = 0$ V is also shown.

at three different fundamental frequencies (2, 10, and 20 MHz) on the selected GaN device under class-A operation and 50-Ω loading condition. It is evident that no major deviations arise by changing the characterization frequency. This confirms the correctness of the chosen frequency (i.e., 2 MHz) to characterize dispersion effects and that negligible uncertainty is introduced by neglecting "faster dynamics" of LF dispersion.[5]

Fig. 3 shows two measurement sets carried out by means of the LF load–pull setup, starting from two different bias conditions $V_g^0 = -4$ V, $V_d^0 = 25$ V (corresponding to class-B operation) and $V_g^0 = -2$ V, $V_d^0 = 25$ V (corresponding to class-A operation). For each set, the different load-lines were obtained by imposing constant amplitude of the gate incident signal (which is chosen to dynamically reach the device output characteristic at $v_g = 0$ V) and sweeping the amplitude of the drain incident signal. The relative phase is maintained constant to 180°. The dc characteristic for $v_g = 0$ V is also reported in order to put in evidence the CC. As can be clearly seen in Fig. 3, the device shows negligible dependence of the KW on the gate bias condition.

[5]This is also confirmed by the large number of papers devoted to GaN device characterization (e.g., [17]), which, for the LF characterization, adopt pulsed measurements setting the pulsewidth to 500 ns or more.

TABLE I
LF MODEL PARAMETERS FOR THE CONSIDERED 0.7-μm GaN HEMT DEVICE

Parameter	*Value*	*Parameter*	*Value*
$\alpha^{m}_{1,0,0}$	0.016 V^{-1}	$\alpha^{g}_{0,2,0}$	0 V^{-1}
$\alpha^{m}_{0,1,0}$	0.017 V^{-1}	$\alpha^{g}_{0,0,2}$	0.0043 $A^{-2}V^{-1}$
$\alpha^{m}_{0,0,1}$	0.059 W^{-1}	$\alpha^{g}_{1,1,0}$	0.00037 V^{-1}
$\alpha^{g}_{1,0,0}$	-0.024	$\alpha^{g}_{1,0,1}$	0.019 W^{-1}
$\alpha^{g}_{0,1,0}$	-0.012	$\alpha^{g}_{0,1,1}$	0.0054 W^{-1}
$\alpha^{g}_{0,0,1}$	-0.077 A^{-1}	$\alpha^{d}_{0,1,0}$	0.025 V^{-1}
$\alpha^{g}_{2,0,0}$	-0.032 V^{-1}		

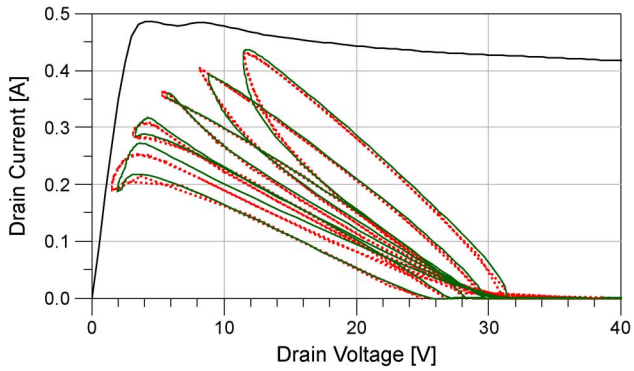

Fig. 4. Measurements (dotted line) carried out on the GaN DUT are compared with model predictions (continuous line). Frequency of operation 2 MHz, class-B bias condition ($V_g^0 = -4$ V, $V_d^0 = 25$ V), amplitude of the input incident signal $A_g = 2$ V, amplitude of the output incident signal 1.4 V $\leq A_d \leq$ 9.8 V, relative phase $\Delta\phi = 180°$.

TABLE II
MODEL PREDICTION OF THE AVERAGE DRAIN CURRENT UNDER DYNAMIC OPERATION ($V_g^0 = -4$ V, $V_d^0 = 25$ V)

A_d *[V]*	*Measured value [mA]*	*Predicted value [mA]*
1.4	127	132
2.6	121	125
4.5	114	118
7.1	101	106
9.8	80	84

Following the guidelines discussed in Section II, the formulation adopted for the considered case study is

$$\begin{aligned}\Delta_m(t) &= \alpha^m_{1,0,0}\delta_{vg} + \alpha^m_{0,1,0}\delta_{vd} + \alpha^m_{0,0,1}\delta_p \\ \Delta_g(t) &= \alpha^g_{1,0,0}\delta_{vg} + \alpha^g_{0,1,0}\delta_{vd} + \alpha^g_{0,0,1}\delta_p \\ &\quad + \alpha^g_{2,0,0}\delta^2_{vg} + \alpha^g_{0,2,0}\delta^2_{vd} + \\ &\quad + \alpha^g_{0,0,2}\delta^2_p + \alpha^g_{1,1,0}\delta_{vg}\delta_{vd} \\ &\quad + \alpha^g_{1,0,1}\delta_{vg}\delta_p + \alpha^g_{0,1,1}\delta_{vd}\delta_p \\ \Delta_d(t) &= \alpha^d_{0,1,0}\delta_{vd} \end{aligned} \quad (12)$$

TABLE III
MODEL PREDICTION OF THD ($V_g^0 = -4$ V, $V_d^0 = 25$ V)

A_d *[V]*	*Measured value [%]*	*Predicted value [%]*
1.4	23.1	22.2
2.6	15.0	14.2
4.5	10.4	10.2
7.1	7.3	7.6
9.8	5.6	6.5

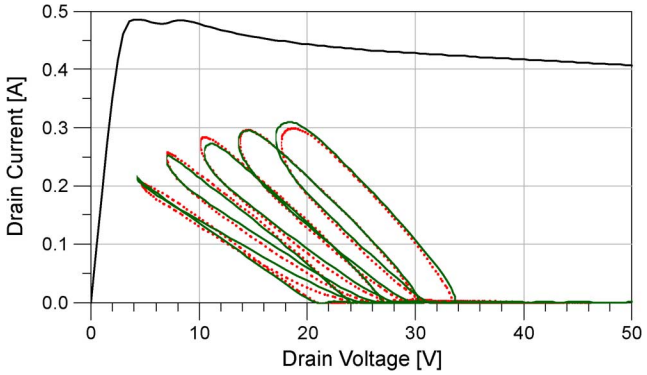

Fig. 5. Measurements (dotted line) performed on the GaN DUT are compared with model predictions (continuous line). Frequency of operation 2 MHz, strong pinchoff bias condition ($V_g^0 = -7$ V, $V_d^0 = 30$ V), amplitude of the input incident signal $A_g = 3.5$ V, amplitude of the output incident signal 1.1 V $\leq A_d \leq$ 9.8 V, relative phase $\Delta\phi = 180°$.

TABLE IV
MODEL PREDICTION OF THE AVERAGE DRAIN CURRENT UNDER DYNAMIC OPERATION ($V_g^0 = -7$ V, $V_d^0 = 30$ V)

A_d *[V]*	*Measured value [mA]*	*Predicted value [mA]*
1.1	56	60
3.2	56	57
5.3	54	54
7.5	50	51
9.8	43	46

TABLE V
MODEL PREDICTION OF THD ($V_g^0 = -7$ V, $V_d^0 = 30$ V)

A_d *[V]*	*Measured value [%]*	*Predicted value [%]*
1.1	60.6	61.6
3.2	32.6	34.4
5.3	21.6	22.5
7.5	14.9	16.0
9.8	9.6	11.6

where, for the gate voltage correction term Δ_g, a second-order polynomial has been found adequate. Moreover, in the drain voltage correction term Δ_d, the contribution deriving from the deviations δ_{vg} has been neglected accordingly to the negligible dependence of the KW on the gate bias condition shown in Fig. 3.

Although the correction technique presented here can be applied to any dc drain current description [27], in this paper,

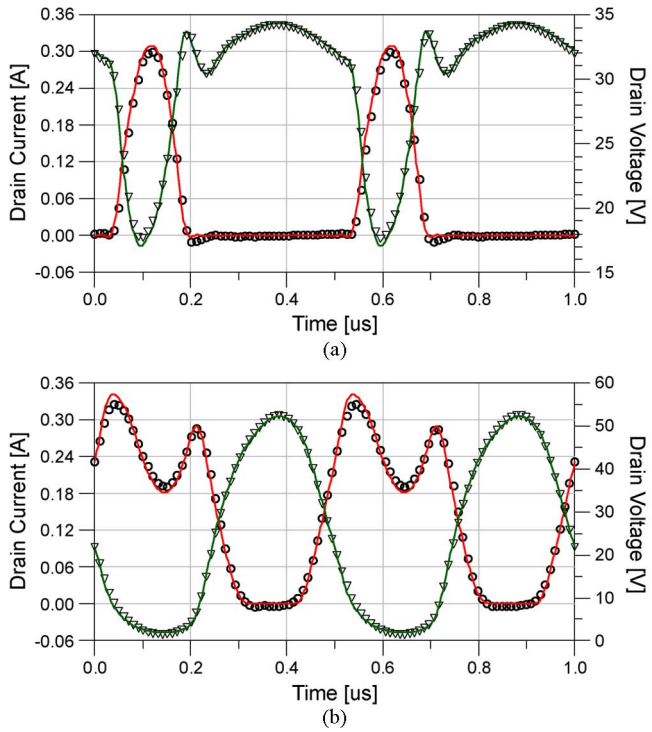

Fig. 6. Measured drain current (circles) and voltage (triangles) compared to respective model predictions (continuous line). (a) $V_g^0 = -7$ V, $V_d^0 = 30$ V, $A_g = 3.5$ V, $A_d = 1.1$ V, and $\Delta\phi = 180°$. (b) $V_g^0 = -2$ V, $V_d^0 = 25$ V, $A_g = 1$ V, $A_d = 11$ V, and $\Delta\phi = 180$.

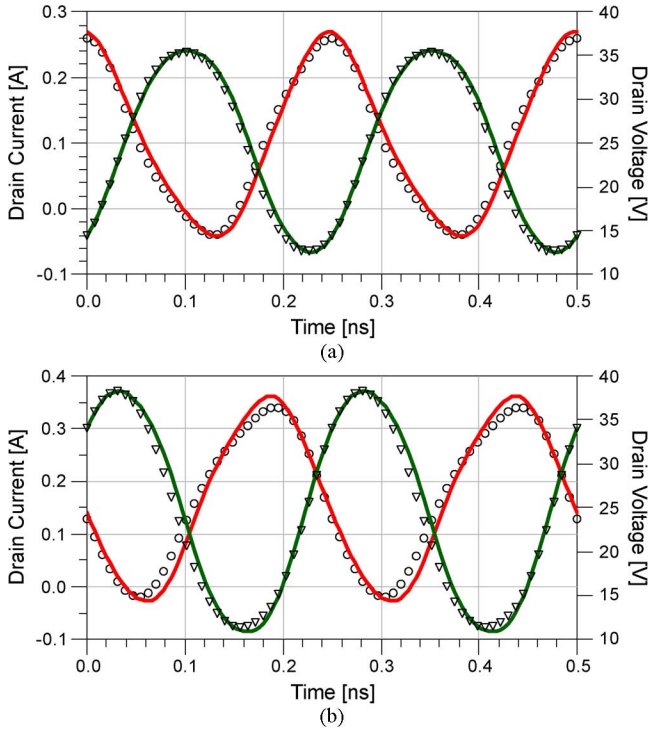

Fig. 7. Active load–pull measurements at 4 GHz. Measured drain current (circles) and voltage (triangles) compared to corresponding model predictions (continuous line). (a) $V_g^0 = -3.25$ V, $V_d^0 = 25$ V, and $Z_L = 71.9 + j * 39.4\ \Omega$. (b) $V_g^0 = -2.25$ V, $V_d^0 = 25$ V, and $Z_L = 66.6 + j * 41.5\ \Omega$.

a look-up-table approach has been used for the static characteristic $F_{\rm dc}$ with the specific aim of quantifying the level of accuracy achievable with the deviation model presented. In particular, this avoids introducing errors related to the static behavior approximation through analytical functions (e.g., smoothing functions and the absence of kink effects, which are instead present in the dc behavior, as shown in Fig. 3).

Two sets of LF measurements were exploited in the identification phase (bias conditions: $V_g^0 = -4$ V, $V_d^0 = 25$ V and $V_g^0 = -3$ V $V_d^0 = 35$ V). The values obtained for the model parameters are reported in Table I.

Fig. 4 compares the model prediction with one of the identification measurement sets, while in Table II, predicted values of the average drain current are listed. As is well known, it is very difficult to correctly estimate such a quantity, which is of critical importance in nonlinear amplifier design. A maximum deviation of 5% is observed here between measurements and predictions.

In Table III, the predicted and measured values of total harmonic distortion (THD) are compared. Also in this case, the agreement is excellent. Identical results were obtained for the other measurement set exploited in the identification phase.

The proposed approach was validated by carrying out several measurements under very different classes of operation to put in evidence the model accuracy.

In Fig. 5, measurements and predictions carried out starting from a strong pinchoff quiescent condition ($V_g^0 = -7$ V, $V_d^0 = 30$ V) are shown. Such a regime of operation strongly emphasizes the influence of trapping states. In fact, the very important KW and CC are well evident. The excellent prediction capability of the developed formulation is also confirmed in Tables IV and V where the comparisons between measured and predicted values of the average drain current and THD are reported. In Fig. 6(a), the time-domain drain waveforms, for the particular case of output incident signal amplitude $A_d = 1.1$ V, are shown: the 40% CC is correctly predicted by the proposed approach.

Fig. 6(b) shows the time-domain drain waveforms for the class-A bias condition ($V_g^0 = -2$ V, $V_d^0 = 25$ V). Also in this case, the high level of prediction accuracy is evident. In particular, in the knee region, the current sinking in correspondence to the voltage minimum peak is perfectly reproduced.

In order to assess the accuracy level obtainable by the proposed approach under high-frequency operation, the identified LF model was embedded into a large-signal device model for microwave applications[6] [32]. To this aim, bias- and frequency-dependent S-parameter measurements were carried out in the frequency range of 40 MHz–40 GHz by means of an Anritsu 37397D vector network analyzer. From a theoretical point of view, dispersion on capacitance should also be accounted for, nevertheless such a type of effect is of minor extent with respect to the dynamic deviations of the drain current. As a matter of fact, capacitance dispersion has been regularly neglected in electron device models oriented to power amplifier design [33], [34].

[6]It is worth noticing that, under high-frequency operation, the term $p(t)$ has to be calculated by considering only the purely algebraic part of the drain current (6).

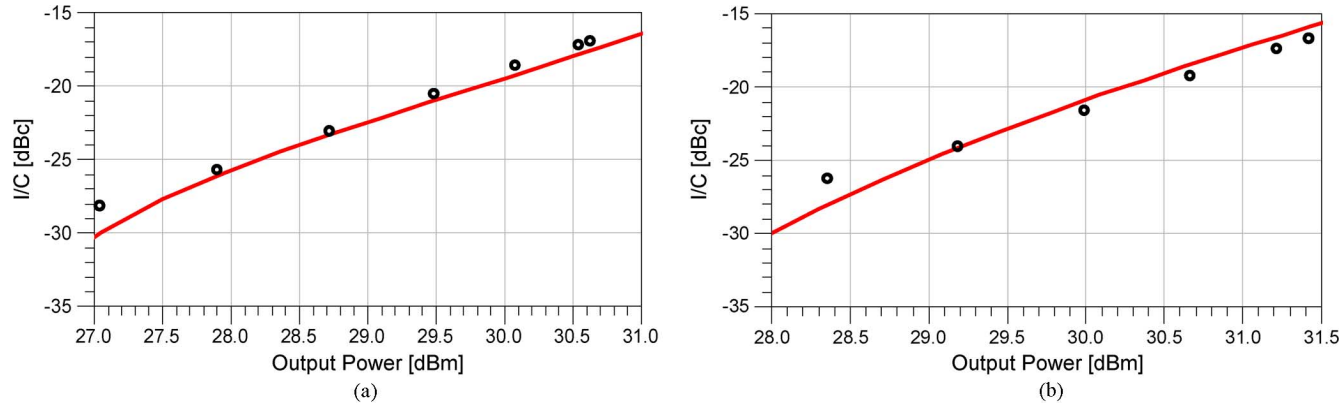

Fig. 8. Third-order I/C versus output power measurements (symbols) carried out at 4 GHz and model predictions (continuous lines) obtained by the proposed formulation. Bias condition $V_g^0 = -2$ V, $V_d^0 = 25$ V, source impedance $Z_S = 9.07 + j * 14.62\ \Omega$ and load impedance: (a) $Z_L = 63.23 + j * 4.63\ \Omega$ and (b) $Z_L = 82.37 + j * 33.93\ \Omega$.

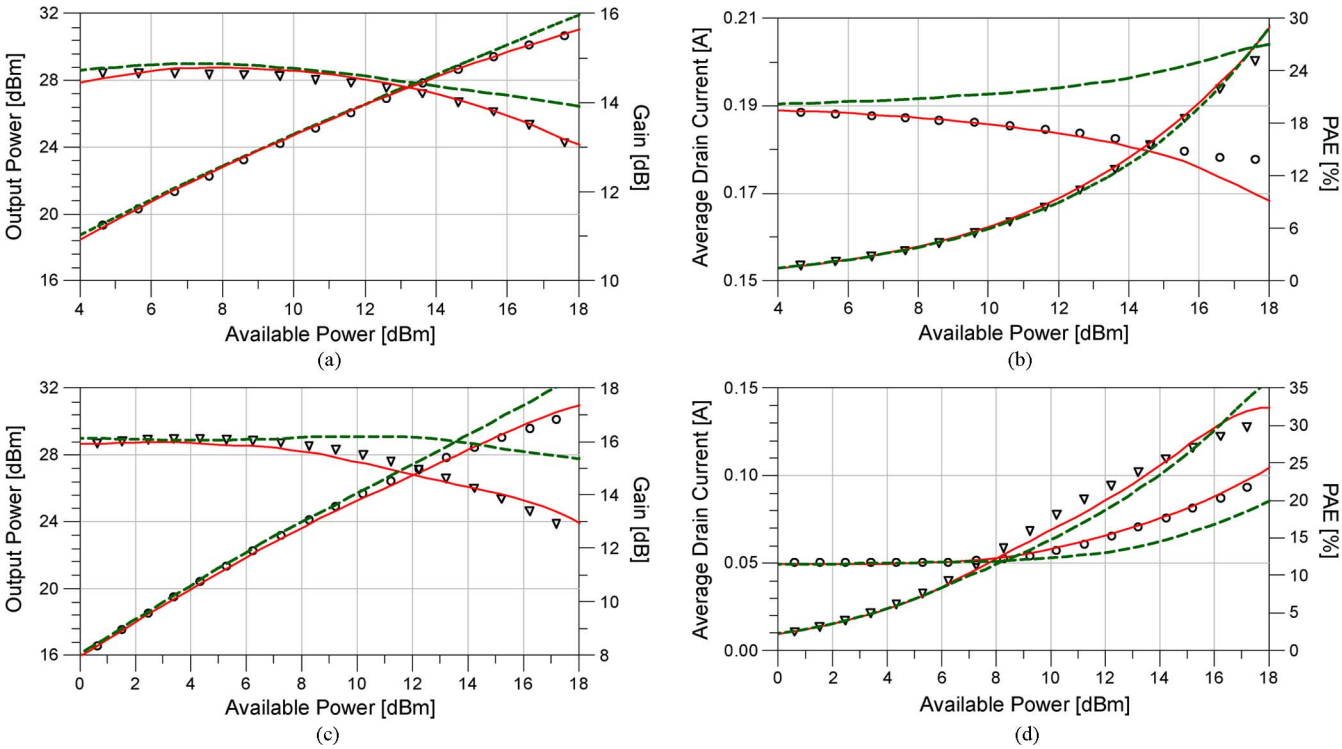

Fig. 9. Comparisons between load–pull measurements (symbols) carried out at 4 GHz and model predictions obtained by the proposed formulation (continuous lines) and a simplified one (dotted lines). Output power (circles), gain (triangles), average drain current (circles), and PAE (triangles). (a) and (b) Bias condition $V_g^0 = -2$ V, $V_d^0 = 25$ V, source impedance $Z_S = 4.56 + j * 8.11\ \Omega$, and load impedance $Z_L = 42.63 + j * 55.02\ \Omega$. (c) and (d) Bias condition $V_g^0 = -3$ V, $V_d^0 = 35$ V, source impedance $Z_S = 11.19 + j * 11.73\ \Omega$, and load impedance $Z_L = 65.89 + j * 98.84\ \Omega$.

The developed approach was validated by exploiting a time-domain load–pull system [13]. More precisely, an active load–pull setup, based on a large-signal network analyzer, has been employed for this study. The drain load was synthesized by sending toward the device output port a power wave, at the fundamental frequency of 4 GHz, with properly controlled amplitude and phase. Moreover, to cover a wide region of the DUT characteristic and synthesize loads close to the edge of the Smith chart, power amplifiers were inserted at the input and output device ports. Also in this context, the model predictions were found in good agreement with measurements under different bias conditions, as clearly shown in Fig. 7.

Load–pull measurements were also carried out by exploiting a 4–26-GHz load–pull system [11], which enables device source and load impedances at the fundamental frequency to be controlled. In particular, third-order intermodulation (IMD) measurements were performed at 4 GHz (tone spacing 10 MHz) under class A operation. In Fig. 8(a) and (b), the level of interferer to carrier ratio (I/C) is shown. The prediction accuracy clearly puts in evidence that the provided description is adequate to accurately model higher order partial derivatives of the nonlinear electrical variables.

Single-tone measurements were also performed at 4 GHz choosing two typical operating conditions: class A [see Fig. 9(a) and (b)] and class AB [see Fig. 9(c) and (d)]. The good agreement obtained between model predictions and measurements for all the considered figures of merit [gain, output power, average drain current, and power-added efficiency (PAE)], as

TABLE VI
SIMPLIFIED MODEL PARAMETERS FOR THE CONSIDERED 0.7-μm GaN HEMT DEVICE

Parameter	*Value*	*Parameter*	*Value*
$\alpha^{m}_{0,0,1}$	0.0022 W^{-1}	$\alpha^{g}_{1,0,0}$	-0.21
$\alpha^{g}_{0,1,0}$	0.0035		

well as the fast simulation times, demonstrates the optimum compromise achievable by adopting the present formulation.

In order to assess the accuracy improvement achieved by (12), Fig. 9 also shows the prediction results obtained through a simplified formulation where only the three correction terms reported in Table VI are considered. This formulation practically coincides with [25] that can be considered representative of models [23]–[27]. The two formulations show the same high accuracy level under small-signal condition. Nevertheless, under nonlinear operation, the improvement deriving from considering additional model parameters is well evident.

IV. CONCLUSION

A very general formulation has been discussed in this paper, which allows to correctly account for LF dispersion affecting FET electron devices. The proposed modeling approach has been validated under very different operations both at low and high frequencies, definitely demonstrating its validity for power amplifier design.

REFERENCES

[1] S. Marsh, *Practical MMIC Design*. Norwood, MA: Artech House, 2006.

[2] M. Albulet, *RF Power Amplifiers*. Atlanta, GA: Noble, 2001.

[3] S. C. Cripps, *RF Power Amplifiers for Wireless Communication*. Norwood, MA: Artech House, 1999.

[4] S. C. Cripps, *Advanced Techniques in RF Power Amplifier Design*. Norwood, MA: Artech House, 2002.

[5] F. Giannini and G. Leuzzi, *Nonlinear Microwave Circuit Design*. Chichester, U.K.: Wiley, 2004.

[6] U. K. Mishra, P. Parikh, and Y.-F. Wu, "AlGaN/GaN HEMTs—An overview of device operation and applications," *Proc. IEEE*, vol. 90, no. 6, pp. 1022–1031, Jun. 2002.

[7] P. Colantonio, F. Giannini, R. Giofre, E. Limiti, A. Serino, M. Peroni, P. Romanini, and C. Proietti, "A C-band high-efficiency second-harmonic-tuned hybrid power amplifier in GaN technology," *IEEE Trans. Microw. Theory Tech.*, vol. 54, no. 6, pp. 2713–2722, Jun. 2006.

[8] M. Helaoui and F. M. Ghannouchi, "Optimizing losses in distributed multiharmonic matching networks applied to the design of an RF GaN power amplifier with higher than 80% power-added efficiency," *IEEE Trans. Microw. Theory Tech.*, vol. 57, no. 2, pp. 314–322, Feb. 2009.

[9] J. M. Cusak, S. M. Perlow, and B. S. Perlman, "Automatic load contour mapping for microwave power transistors," *IEEE Trans. Microw. Theory Tech.*, vol. 22, no. 12, pp. 1146–1152, Dec. 1974.

[10] A. Ferrero and V. Teppati, "Accuracy evaluation of on-wafer load–pull measurements," in *Proc. IEEE 55th ARFTG Microw. Meas. Conf.*, Boston, MA, 2000, pp. 1–5.

[11] *"Focus Microwaves Data Manual,"* Focus Microw. Inc., Montreal, QC, Canada, 1988.

[12] M. N. Tutt, D. Pavlidis, and C. Tsironis, "Automated on-wafer noise and load pull characterization using precision computer controlled electromechanical tuners," in *Proc. IEEE 37th ARFTG Microw. Meas. Conf.*, Boston, MA, 1991, pp. 66–75.

[13] D. Schreurs, K. Van der Zanden, J. Verspecht, W. De Raedt, and B. Nauwelaers, "Real-time measurement of InP HEMTs during large-signal RF overdrive stress," in *Proc. Eur. Gallium Arsenide Related III–V Compounds Appl. Symp.*, Amsterdam, The Netherlands, 1998, pp. 545–550.

[14] F. De Groote, J.-P. Teyssier, O. Jardel, T. Gasseling, and J. Verspecht, "Introduction to measurements for power transistor characterization," *IEEE Microw. Mag.*, vol. 9, no. 3, pp. 70–85, Jun. 2008.

[15] J. Rodriguez-Tellez, T. Fernandez, A. Mediavilla, and A. Tazon, "Characterization of thermal and frequency-dispersion effects in GaAs MESFET devices," *IEEE Trans. Microw. Theory Tech.*, vol. 49, no. 7, pp. 1352–1355, Jul. 2001.

[16] P. McGovern, J. Benedikt, P. J. Tasker, J. Powell, K. P. Hilton, J. L. Glasper, R. S. Balmer, T. Martin, and M. J. Uren, "Analysis of DC–RF dispersion in AlGaN/GaN HFETs using pulsed *I–V* and time-domain waveform measurements," presented at the IEEE MTT-S Int. Microw. Symp., Long Beach, CA, 2005.

[17] W. Ciccognani, F. Giannini, E. Limiti, P. E. Longhi, M. A. Nanni, A. Serino, C. Lanzieri, M. Peroni, P. Romanini, V. Camarchia, M. Pirola, and G. Ghione, "GaN device technology: Manufacturing, characterization, modelling and verification," in *Proc. IEEE 14th Microw. Tech. Conf.*, Prague, Czech Republic, 2008, pp. 1–6.

[18] S. Augaudy, R. Quere, J. P. Teyssier, M. A. Di Forte-Poisson, S. Cassette, B. Dessertenne, and S. L. Delage, "Pulse characterization of trapping and thermal effects of microwave GaN power FETs," in *IEEE MTT-S Int. Microw. Symp. Dig.*, Phoenix, AZ, May 2001, pp. 427–430.

[19] C. Fiegna, F. Filicori, G. Vannini, and F. Venturi, "Modeling the effects of traps on the I–V characteristics of GaAs MESFETs," in *Proc. IEEE Int. Electron Devices Meeting*, Washington, DC, Dec. 1995, pp. 773–776.

[20] C. Camacho-Penalosa, "Modeling frequency dependence of output impedance of a microwave MESFET at low frequencies," *Electron. Lett.*, vol. 21, no. 12, pp. 528–529, Jun. 1985.

[21] F. Filicori, G. Vannini, A. Santarelli, A. M. Sanchez, A. Tazon, and Y. Newport, "Empirical modeling of low-frequency dispersive effects due to traps and thermal phenomena in III–V FET's," *IEEE Trans. Microw. Theory Tech.*, vol. 43, no. 12, pp. 2972–2981, Dec. 1995.

[22] A. Raffo, A. Santarelli, P. A. Traverso, M. Pagani, F. Palomba, F. Scappaviva, G. Vannini, and F. Filicori, "Accurate PHEMT nonlinear modeling in the presence of low-frequency dispersive effects," *IEEE Trans. Microw. Theory Tech.*, vol. 53, no. 11, pp. 3449–3459, Nov. 2005.

[23] A. Raffo, V. Vadalà, G. Vannini, and A. Santarelli, "A new empirical model for the characterization of low-frequency dispersive effects in FET electron devices accounting for thermal influence on the trapping state," in *IEEE MTT-S Int. Microw. Symp. Dig.*, Atlanta, GA, 2008, pp. 1421–1424.

[24] K. Jeon, Y. Kwon, and S. Hong, "A frequency dispersion model of GaAs MESFET for large-signal applications," *IEEE Microw. Guided Wave Lett.*, vol. 7, no. 3, pp. 78–80, Mar. 1997.

[25] A. Santarelli, G. Vannini, F. Filicori, and P. Rinaldi, "Backgating model including self-heating for low-frequency dispersive effects in III–V FETs," *Electron. Lett.*, vol. 34, no. 20, pp. 1974–1976, Oct. 1998.

[26] M. Chaibi, T. Fernandez, J. Rodriguez-Tellez, J. L. Cano, and M. Aghoutane, "Accurate large-signal single current source thermal model for GaAs MESFET/HEMT," *IEEE Electron. Lett.*, vol. 43, no. 14, p. , Jul. 2007.

[27] M. Chaibi, T. Fernandez, J. R. Tellez, A. Tazon, and M. Aghoutane, "Modelling of temperature and dispersion effects in MESFET and HEMT transistors," in *Proc. IEEE Integr. Nonlinear Microw. Millimeter-Wave Circuits Workshop*, Malaga, Spain, 2008, pp. 173–175.

[28] T. Roh, Y. Kim, Y. Suh, W. Park, and B. Kim, "A simple and accurate MESFET channel-current model including bias-dependent dispersion and thermal phenomena," *IEEE Trans. Microw. Theory Tech.*, vol. 45, no. 8, pp. 1252–1255, Aug. 1997.

[29] O. Jardel, F. De Groote, T. Reveyrand, J.-C. Jacquet, C. Charbonniaud, J.-P. Teyssier, D. Floriot, and R. Quere, "An electrothermal model for AlGaN/GaN power HEMTs including trapping effects to improve large-signal simulation results on high VSWR," *IEEE Trans. Microw. Theory Tech.*, vol. 55, no. 12, pp. 2660–2669, Dec. 2007.

[30] I. Angelov and C. Karnfelt, "Direct extraction techniques for thermal resistance of MESFET and HEMT devices," in *Proc. IEEE Radio Freq. Integr. Circuits Symp.*, Honolulu, HI, 2007, pp. 351–354.

[31] A. Raffo, V. Vadalà, P. A. Traverso, A. Santarelli, G. Vannini, and F. Filicori, "An innovative two-source large-signal measurement system for the characterization of low-frequency dispersive effects in FETs," in *Proc. 16th Int. Meas. Confederation TC4 Symp.*, Florence, Italy, 2008, pp. 72–77.

[32] G. Crupi, D. M. M.-P. Schreurs, D. Xiao, A. Caddemi, B. Parvais, A. Mercha, and S. Decoutere, "Determination and validation of new nonlinear FinFET model based on lookup tables," *IEEE Microw. Wireless Compon. Lett.*, vol. 17, no. 5, pp. 361–363, May 2007.
[33] I. Angelov, N. Rorsman, J. Stenarson, M. Garcia, and H. Zirath, "An empirical table-based FET model," *IEEE Trans. Microw. Theory Tech.*, vol. 47, no. 12, pp. 2350–2357, Dec. 1999.
[34] M. Fernández-Barciela, P. J. Tasker, Y. Campos-Roca, M. Demmler, H. Massler, E. Sanchez, M. C. Curras-Francos, and M. Schlechtweg, "A simplified broadband large signal non quasi-static table-based FET model," *IEEE Trans. Microw. Theory Tech.*, vol. 48, no. 3, pp. 395–405, Mar. 2000.

Antonio Raffo (S'04–M'07) was born in Taranto, Italy, in 1976. He received the M.S. degree (with honors) in electronic engineering and Ph.D. degree in information engineering from the University of Ferrara, Ferrara, Italy, in 2002 and 2006, respectively.

Since 2002, he has been with the Department of Engineering, University of Ferrara, where he is currently a Contract Professor of electronic instrumentation and measurement. His research activity is mainly oriented to nonlinear electron device characterization and modeling and circuit-design techniques for nonlinear microwave and millimeter-wave applications.

Dr. Raffo is a member of the Italian Association on Electrical and Electronic Measurements.

Valeria Vadalà (S'07) was born in Reggio Calabria, Italy, in 1982. She received the M.S. degree (with honors) in electronic engineering from the "Mediterranea" University of Reggio Calabria, Reggio Calabria, Italy, in 2006, and is currently working toward the Ph.D. degree at the University of Ferrara, Ferrara, Italy.

She is currently with the Department of Engineering, University of Ferrara, and also collaborates with the Department of Electronics, University of Bologna. Her research interests include nonlinear electron-device characterization and modeling for microwave applications.

Dominique M. M.-P. Schreurs (S'90–M'97–SM'02) received the M.Sc. degree in electronic engineering and Ph.D. degree from the Katholieke Universiteit (K.U.) Leuven, Leuven, Belgium.

She is currently an Associate Professor with K.U. Leuven. She has been a Visiting Scientist with Agilent Technologies, Eidgenössische Technische Hochschule Zürich (ETH Zürich), and the National Institute of Standards and Technology (NIST). Her main research interests concern the (non)linear characterization and modeling of active microwave devices, and (non)linear hybrid and integrated circuit design.

Dr. Schreurs serves on the IEEE Microwave Theory and Techniques Society (IEEE MTT-S) Administrative Committee (AdCom). She is vice-chair of the IEEE MTT-S Technical Coordinating Committee, and past chair of the Technical Committee on microwave measurements (MTT-11). She also serves as education chair on the Executive Committee of the ARFTG organization, and was general chair of the 2007 Spring ARFTG Conference. She was also workshop coordinator of European Microwave Week (EuMW) and co-chair of the European Microwave Conference (EuMC) in 2008.

Giovanni Crupi was born in Lamezia Terme, Italy, in 1978. He received the M.Sc. degree (*cum laude*) in electronic engineering and Ph.D. degree from the University of Messina, Messina, Italy, in 2003 and in 2006, respectively.

He is currently a Contract Researcher with the Dipartimento di Fisica della Materia e Ingegneria Elettronica, University of Messina, where he holds the course of "Optoelectronics." Since 2005, he has been a repeat Visiting Scientist with the Katholieke Universiteit (K.U.) Leuven, Leuven, Belgium, and the Interuniversity Microelectronics Center (IMEC), Leuven, Belgium. His main research interests include small- and large-signal modeling of advanced microwave devices.

Gustavo Avolio was born in Cosenza, Italy, in 1982. He received the MSc. degree in electronic engineering from the University of Calabria, Calabria, Italy, in 2006, and is currently working toward the Ph.D. degree at the Katholieke Universiteit (K.U.) Leuven, Leuven, Belgium.

In January 2008, he joined the TELEMIC Division, K.U. Leuven. His research focuses on large-signal measurements and nonlinear modeling of advanced microwave devices.

Alina Caddemi received the Electronic Engineering degree (with honors) and Ph.D. degree from the University of Palermo, Palermo, Italy, in 1982 and in 1987, respectively.

In 1984, she joined the Electrical Engineering Department, University of Utah, Salt Lake City, as a Visiting Researcher. In 1985, she joined the Electrical and Computer Engineering Department, University of Colorado at Boulder, as a Visiting Researcher. From 1990 to 1998, she was with the Department of Electrical Engineering, University of Palermo, as an Assistant Professor. In 1998, she joined the University of Messina, Messina, Italy, as an Associate Professor of electronics. Her current research interests are in the field of temperature-dependent linear and noise characterization techniques for solid-state devices, cryogenic measurements and modeling of FETs and HEMTs, noise modeling of bipolar and FETs for hybrid microwave integrated circuit (HMIC) and monolithic microwave integrated circuit (MMIC) design, neural network and genetic algorithm modeling of devices, design and realization of hybrid low-noise circuits based on either conventional and superconductive materials, characterization, and modeling of thin-film sensors.

Giorgio Vannini (S'87–M'92) received the Laurea degree in electronic engineering and Ph.D. degree in electronic and computer science engineering, from the University of Bologna, Bologna, Italy, in 1987 and 1992, respectively.

In 1992, he joined the Department of Electronics, University of Bologna, as a Research Associate. From 1994 to 1998, he was with the Research Centre on Electronics, Computer science and Telecommunication Engineering, National Research Council (CSITE), Bologna, Itlay, where he was responsible for the Monolithic Microwave Integrated Circuit (MMIC) Testing and Computer-Aided Design (CAD) Laboratory. In 1998, he joined the University of Ferrara, Ferrara, Italy, as an Associate Professor, and since 2005, as a Full Professor of electronics. he is currently Head of the Engineering Department, University of Ferrara. During his academic career, he has been a Teacher of applied electronics, electronics for communications, and industrial electronics. He is a cofounder of the academic spin-off Microwave Electronics for Communications (MEC). He has coauthored over 170 papers devoted to electron device modeling, computer-aided design techniques for MMICs, and nonlinear circuit analysis and design.

Dr. Vannini is a member of the Gallium Arsenide Application Symposium (GAAS) Association. He was the recipient of the Best Paper Award presented at the 25th European Microwave Conference and GAAS98 and GAAS2001 conferences.